Supporting Information for

Adjacent effect between Gd(III) and Cu(II) in layered double hydroxide nanoparticles synergistically enhances T_1-weighted magnetic resonance imaging contrast

Jianping Liu,[a] *Li, Li,*[a] *Run Zhang,*,*[a] *Zhi Ping Xu*,*[a,b]

[a] Australian Institute for Bioengineering and Nanotechnology (AIBN), The University of Queensland, St Lucia, QLD 4072, Australia.

[b] Institute of Biomedical Health Technology and Engineering and Institute of Systems and Physical Biology, Shenzhen Bay Laboratory. Shenzhen, P. R. China 518107.

* Corresponding authors.

Email: gordonxu@uq.edu.au (Z. P. Xu); r.zhang@uq.edu.au (R. Zhang)

1. Supporting Figures

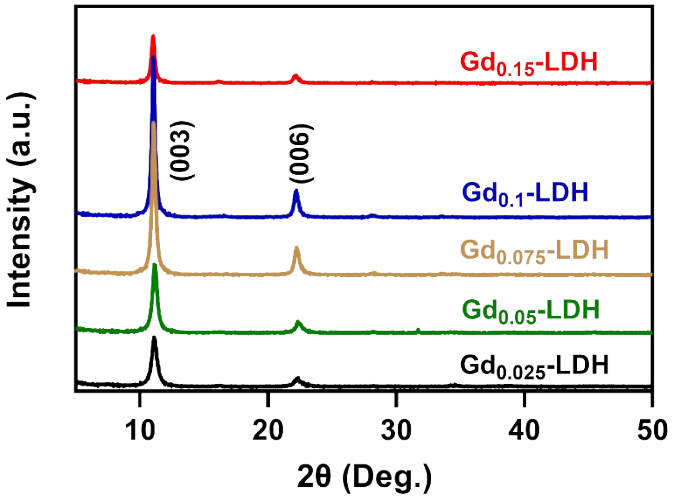

Fig. S1. XRD patterns of a series of Gd_x-LDH.

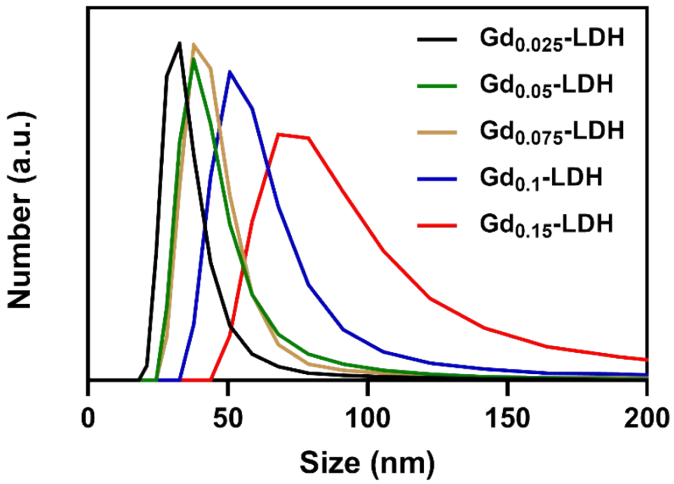

Fig. S2. Size distributions of a series of Gd_x-LDH.

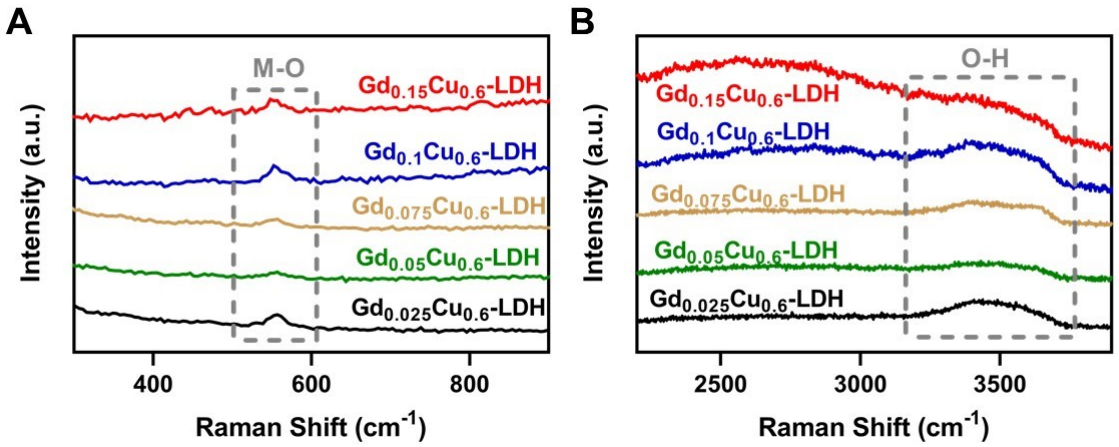

Fig. S3. Raman spectra of a series of $Gd_xCu_{0.6}$-LDH with the wavelength (A) 300-900 cm^{-1} and (B) 2200-3900 cm^{-1}.

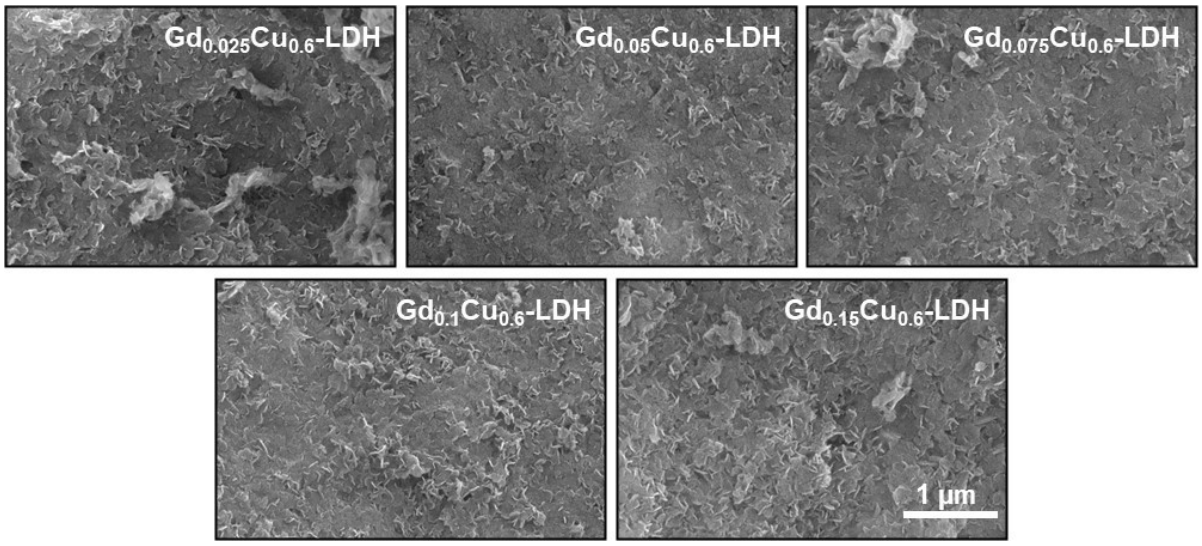

Fig. S4. SEM images of a series of $Gd_xCu_{0.6}$-LDH.

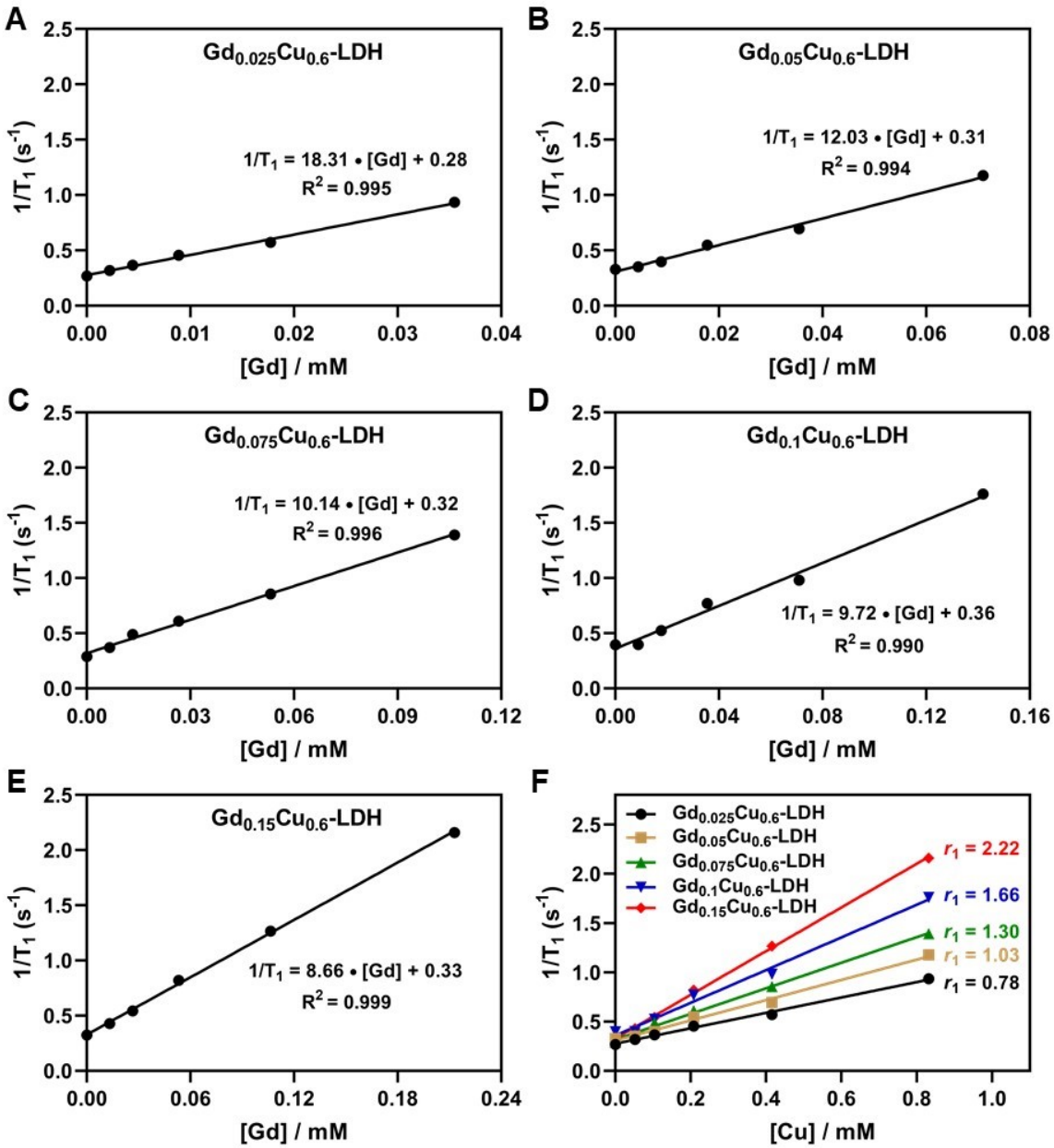

Fig. S5. T_1-weight relaxation of $Gd_xCu_{0.6}$-LDH. Plot of $1/T_1$ versus (A-E) Gd concentration and (F) Cu concentration of a series of $Gd_xCu_{0.6}$-LDH.

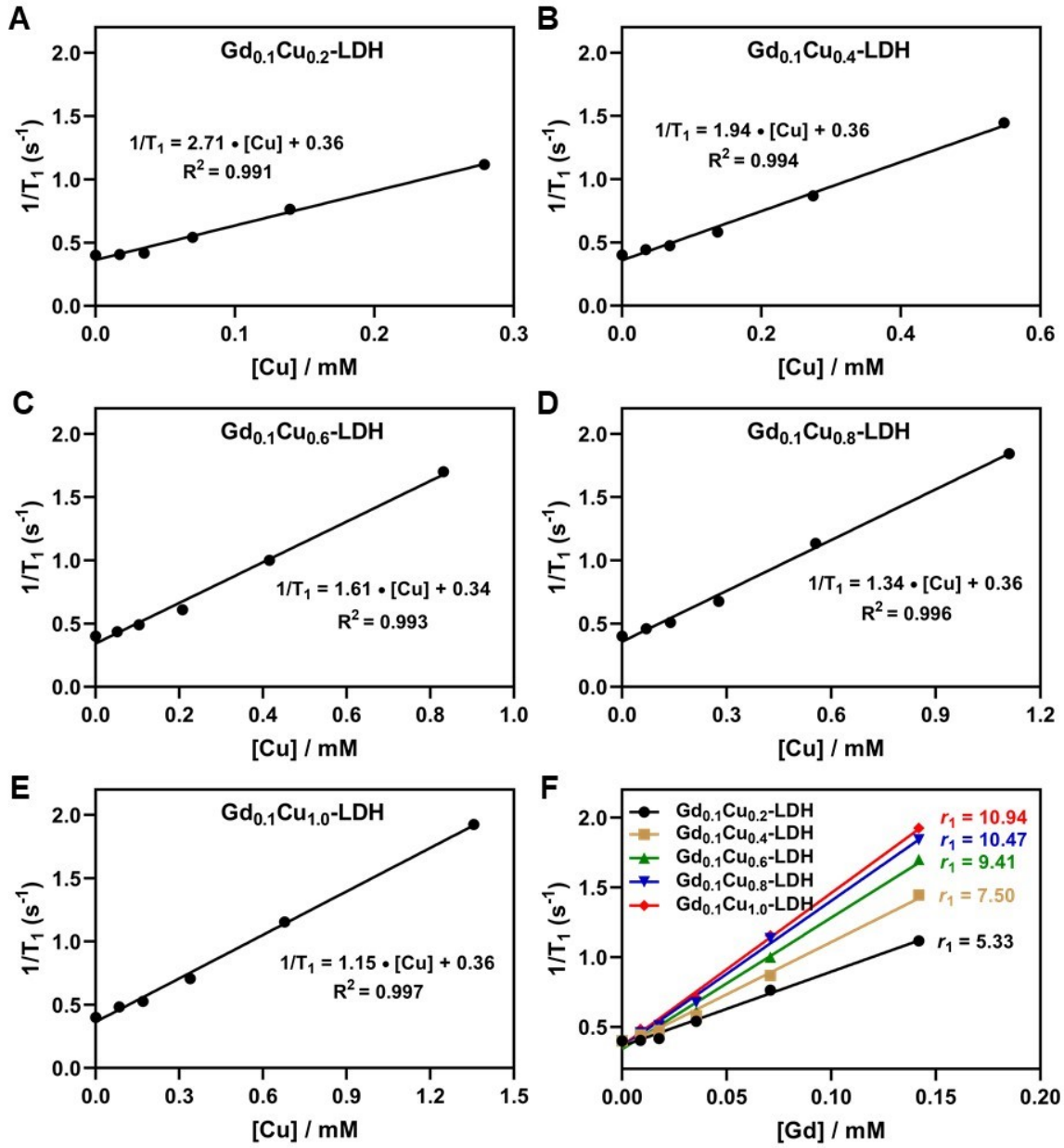

Fig. S6. T_1-weight relaxation of $Gd_{0.1}Cu_y$-LDH. Plot of $1/T_1$ versus (A-E) Cu concentration and (F) Gd concentration of a series of $Gd_{0.1}Cu_y$-LDH.

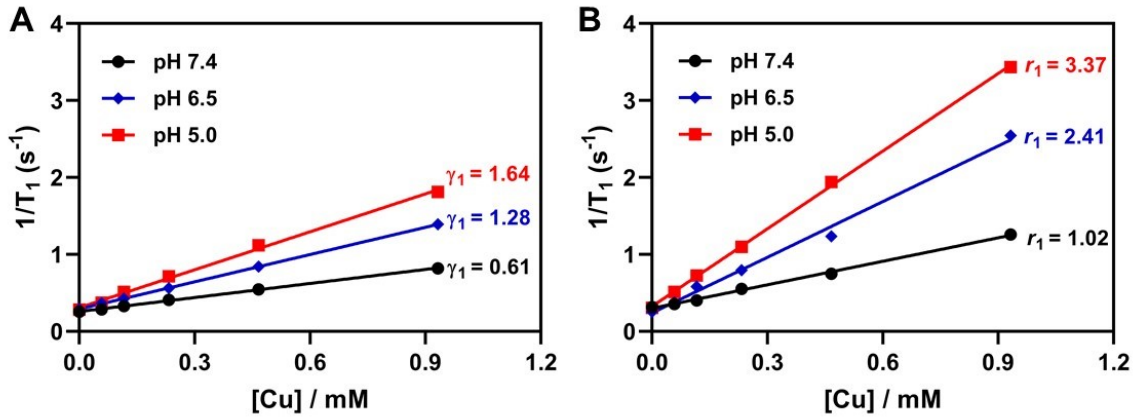

Fig. S7. pH-dependent MRI performance. Plot of $1/T_1$ versus Cu concentration of (A) Cu-LDH and (B) GdCu-LDH (in terms of [Cu]) after co-incubation in different pH buffer solutions for 4 h.

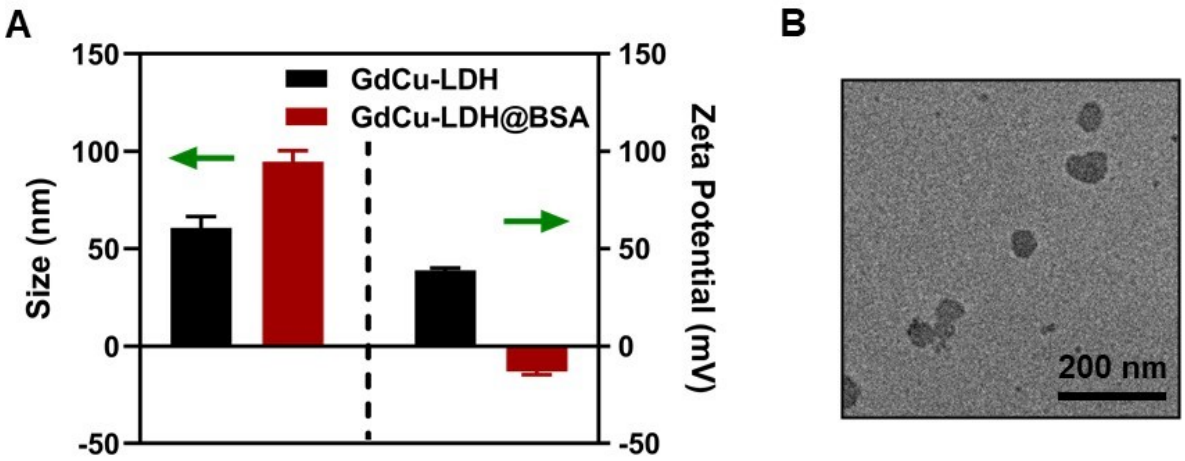

Fig. S8. (A) Particle size and zeta potential of GdCu-LDH and GdCu-LDH@BSA. (B) TEM image of GdCu-LDH@BSA.

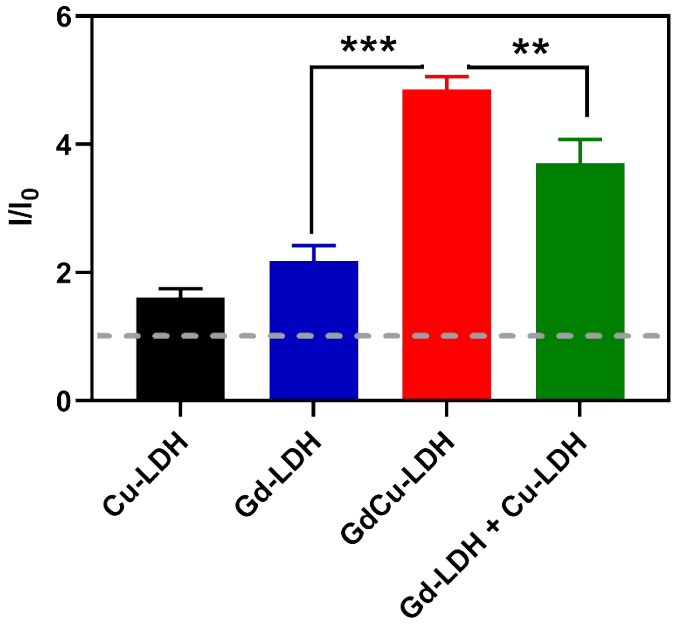

Fig. S9. MRI signal intensity of Cu-LDH, Gd-LDH, GdCu-LDH and analyzed Gd-LDH + Cu-LDH at 24 h post iv injection. I_0 and I: MRI signal intensity of the mice tumors before injection and at 24 h point post injection, respectively. Grey dash line represents the background MRI signal intensity. **: $p < 0.01$; ***: $p < 0.001$.

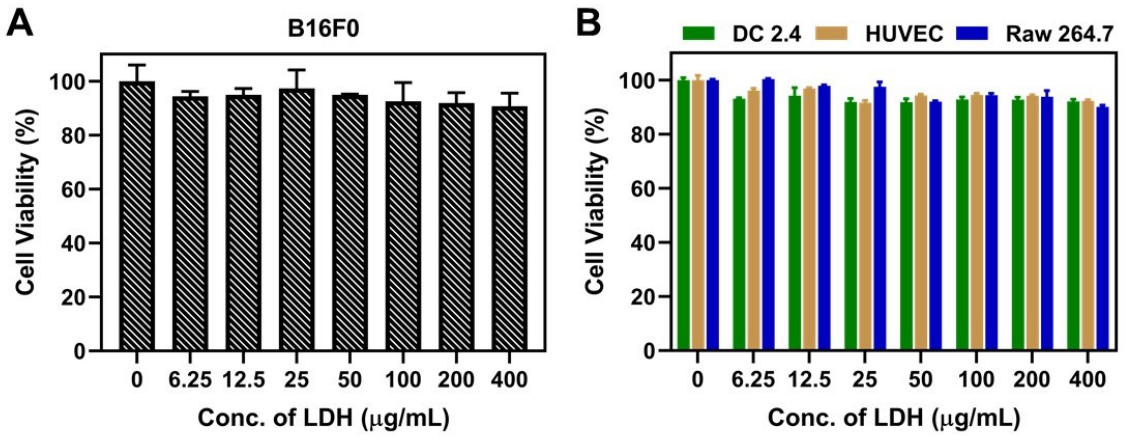

Fig. S10. Cytotoxicity evaluation of GdCu-LDH in B16F0 cells (A) and normal cells (B).

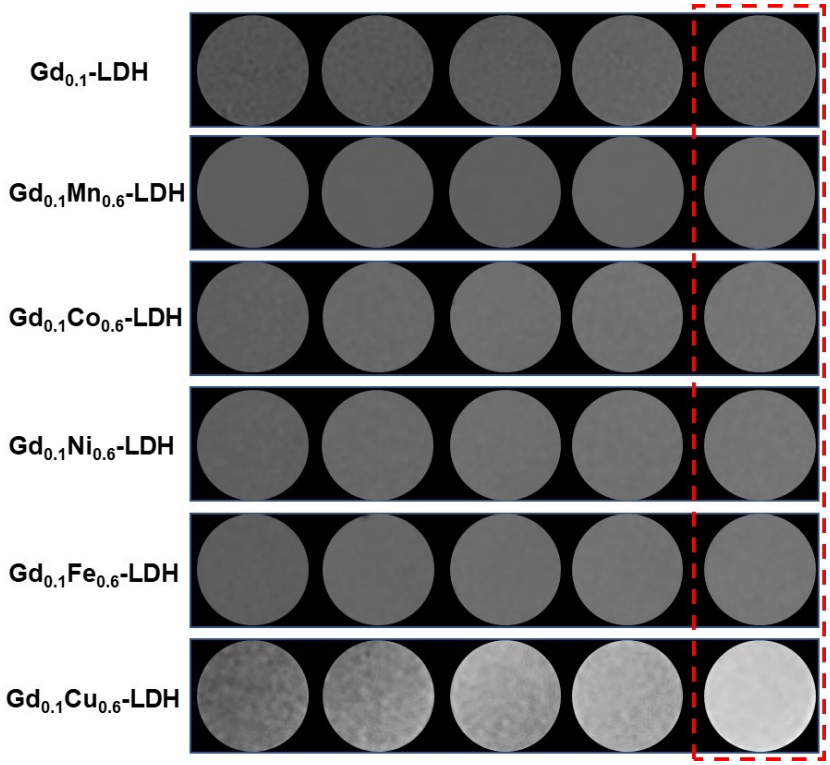

Fig. S11. T_1-weighted MR images of $Gd_{0.1}M_{0.6}$-LDH (M = Mn, Co, Ni, Fe, Cu).

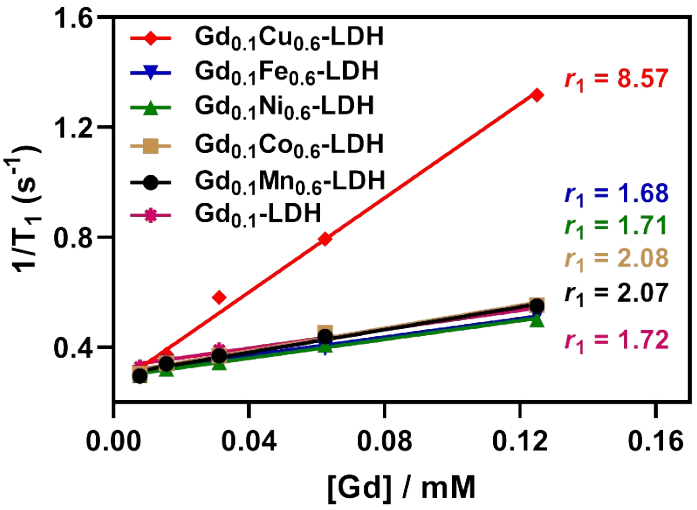

Fig. S12. Plot of $1/T_1$ versus Gd concentration of $Gd_{0.1}M_{0.6}$-LDH (M = Mn, Co, Ni, Fe, Cu).

2. Supporting Tables

Table S1. Particle size, zeta potential, (003) position and element composition of Gd_x-LDH (x = 0.025, 0.05, 0.075, 0.1, and 0.15).

Samples	Size (nm)	Zeta (mV)	Position 2θ (°)	Calculated Chemical Formula
$Gd_{0.025}$-LDH	35.6	36.7	11.12	$Mg_3Al_{0.974}Gd_{0.026}(OH)_{8.0}Cl_{1.0}$
$Gd_{0.05}$-LDH	45.3	31.7	11.15	$Mg_3Al_{0.948}Gd_{0.052}(OH)_{8.0}Cl_{1.0}$
$Gd_{0.075}$-LDH	45.7	38.2	11.07	$Mg_3Al_{0.925}Gd_{0.075}(OH)_{8.0}Cl_{1.0}$
$Gd_{0.1}$-LDH	63.7	36.2	11.05	$Mg_3Al_{0.898}Gd_{0.102}(OH)_{8.0}Cl_{1.0}$
$Gd_{0.15}$-LDH	94.2	32.6	11.03	$Mg_3Al_{0.847}Gd_{0.153}(OH)_{8.0}Cl_{1.0}$

Table S2. Particle size, zeta potential, (003) 2θ value and element composition of $Gd_xCu_{0.6}$-LDH.

Samples	Size (nm)	Zeta (mV)	Position 2θ (°)	Calculated Chemical Formula
$Gd_{0.025}Cu_{0.6}$-LDH	50.5	36.9	11.07	$Mg_{2.46}Al_{0.974}Gd_{0.026}Cu_{0.54}(OH)_{8.0}Cl_{1.0}$
$Gd_{0.05}Cu_{0.6}$-LDH	52.2	39.7	11.15	$Mg_{2.42}Al_{0.948}Gd_{0.052}Cu_{0.58}(OH)_{8.0}Cl_{1.0}$
$Gd_{0.075}Cu_{0.6}$-LDH	56.0	30.3	11.07	$Mg_{2.45}Al_{0.925}Gd_{0.075}Cu_{0.55}(OH)_{8.0}Cl_{1.0}$
$Gd_{0.1}Cu_{0.6}$-LDH	58.4	34.0	11.07	$Mg_{2.42}Al_{0.898}Gd_{0.102}Cu_{0.58}(OH)_{8.0}Cl_{1.0}$
$Gd_{0.15}Cu_{0.6}$-LDH	129	34.8	11.01	$Mg_{2.43}Al_{0.847}Gd_{0.153}Cu_{0.57}(OH)_{8.0}Cl_{1.0}$